ELSEVIER

Applied Surface Science 197–198 (2002) 904–910

applied surface science

www.elsevier.com/locate/apsusc

Resonance and steep fronts effects in nanosecond dry laser cleaning

N. Arnold*

Angewandte Physik, Johannes-Kepler-Universität, Altenbergerstrasse 69, A-4040 Linz, Austria

Abstract

A dynamic model for nanosecond dry laser cleaning (DLC) is discussed. Formulas for the time-dependent thermal expansion of the substrate, valid for temperature-dependent parameters are given. Van der Waals adhesion, the elasticity of the substrate and particle, as well as particle inertia are taken into account for an arbitrary temporal profile of the laser pulse. Time scale related to the size of the particles and to the adhesion/elastic constants is revealed. Cleaning proceeds in different regimes if the duration of the laser pulse and its edges are much shorter/longer than this characteristic time. Utilization of resonance effects and steep fronts of cleaning pulse are suggested. Simple expressions for cleaning thresholds are discussed. Numerical results are presented for the cleaning of Si surfaces from spherical SiO_2 particles.

Keywords: Laser cleaning; Modeling; Adhesion; Oscillations; SiO_2; Si

1. Introduction

Laser cleaning [1] is under consideration for many manufacturing processes [2,3]. In dry laser cleaning (DLC), one usually compares cleaning and adhesion forces [4–6]. Recently, it has been realized that nanosecond DLC requires consideration of dynamic effects [7–11]. Using the approach introduced in [8,9], we discuss the influence of experimental parameters on DLC, and make experimental suggestions. In particular, usage of laser pulses with steep fronts and periodic modulation of intensity may improve DLC.

2. Theoretical framework: adhesion potential, evolution equation, and thermal expansion

Recently, we formulated laser cleaning problem as an escape from the potential under the action of a time-dependent force [8,9]. Main results can be summarized as follows. Particle with the radius r and a plane, approach by a distance h (see Fig. 1). Approximate potential and force that take into account Van der Waals attraction and elastic energy [12] are

$$U = -2\pi rh\varphi + h^{5/2}r^{1/2}(\tfrac{2}{5}\bar{E}),$$
$$F = 2\pi r\varphi - h^{3/2}r^{1/2}\bar{E}, \tag{1}$$

where φ is the work of adhesion (over the contact area $2\pi rh$) and $(1/\bar{E}) = 3/4((1-\sigma^2)/E + (1-\sigma_p^2)/E_p)$ characterizes elastic properties of the substrate and the particle (index "p"). E is Young's modulus and σ the Poisson's ratio. Equilibrium values of h_0 and U_0 are

$$h_0 = \left(\frac{2\pi\varphi}{\bar{E}}\right)^{2/3} r^{1/3}, \quad U_0 = -\tfrac{3}{5}(2\pi\varphi)^{5/3}\bar{E}^{-2/3}r^{4/3}. \tag{2}$$

Detachment occurs when $h = 0$ and requires pull-out force $F_0 = 2\pi r\varphi$. Parabolic approximation to the

* Tel.: +43-732-2468-9245; fax: +43-732-2468-9242.
E-mail address: nikita.arnold@jku.at (N. Arnold).

0169-4332/02/$ – see front matter
PII: S0169-4332(02)00453-1

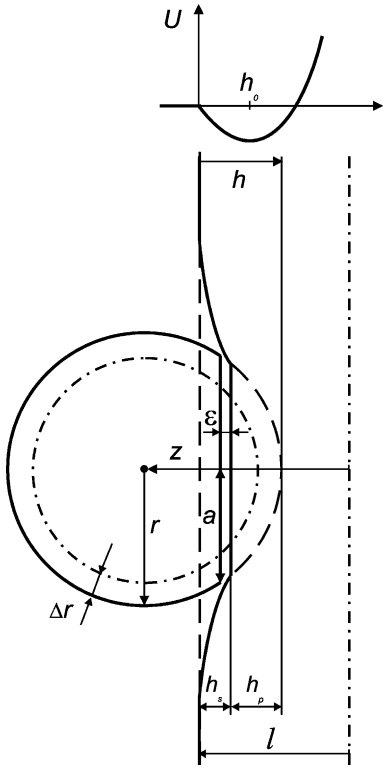

Fig. 1. Schematic of the particle–substrate deformation. Solid lines: boundaries of substrate and particles; dashed lines: imaginary non-deformed boundaries; dash-dotted lines: initial position of the substrate and not heated (but displaced) particle; l: substrate displacement; r: current particle radius; Δr: particle expansion; z: position of the particle center referred to initial (non-deformed) substrate; h: total deformation; h_p and h_s: fractions of total deformation belonging to the substrate and the particle; a: contact radius; ε: equilibrium distance between adhering surfaces. Adhesion potential $U(h)$ is shown schematically.

potential in Eq. (1) yields frequency and period of small oscillations:

$$\omega_0 = \frac{3}{5^{1/2}(2\pi)^{1/3}}\left(\frac{\varphi\bar{E}^2}{r^7\rho_p^3}\right)^{1/6} \sim \left(\frac{v_s^4\varphi}{r^7\rho}\right)^{1/6} \sim 0.5\times 10^9\,\mathrm{s}^{-1}, \quad \tau_0 = \frac{2\pi}{\omega_0} \sim 10\,\mathrm{ns}, \tag{3}$$

where v_s is the sound velocity. Estimations assume $r \sim 1$ μm and material parameters from the Table 1.

Let l be the surface displacement in the laboratory frame. Then Newton's equation, with the force from Eq. (1) in the reference frame fixed with the substrate, reads (dot stands for time derivative and m is the particle mass):

$$\ddot{h} = -\frac{1}{m}\frac{\partial U}{\partial h} + \ddot{l}. \tag{4}$$

Expansion of the particle and damping can be included into consideration [8,9]. We consider here only quasi-static unilateral expansion of the substrate relevant for nanosecond DLC. Surface displacement l and velocity are given by

$$l(t) = \frac{1+\sigma}{1-\sigma}\frac{\beta\phi_a(t)}{3c\rho}, \quad \dot{l} = \frac{1+\sigma}{1-\sigma}\frac{\beta I_a(t)}{3c\rho}, \tag{5}$$

where ϕ_a and I_a are the absorbed fluence and intensity. Excimer laser pulse is approximated by

$$I(t) = I_0\frac{t}{\tau}\exp\left(-\frac{t}{\tau}\right). \tag{6}$$

With this definition $\phi = I_0\tau$, and the full widths half maximum (FWHM) pulse duration $\tau_{FWHM} \approx 2.45\tau$.

3. Cleaning threshold for a single pulse

If the pulse is short, i.e. $\tau \ll \tau_0$, cleaning force $\ddot{l}$ dominates during the pulse. Neglecting the potential in Eq. (4) we obtain

$$\dot{h} \approx \dot{l} \quad \Rightarrow \quad h(\tau) \approx h_0 + l, \quad \dot{h}(\tau) \approx 0. \tag{7}$$

Here, l is the total thermal expansion of the substrate. Thus, energy acquired at the end of the pulse is due to change in h (deformation). Cleaning will take place (after the pulse) if the accumulated (potential) energy is higher than the detachment energy—'elastic energy' cleaning regime. This results in:

$$U(h_0 + l) > 0 \quad \Rightarrow \quad l > \left(\left(\frac{5}{2}\right)^{2/3} - 1\right)h_0 \approx 0.84h_0. \tag{8}$$

If the pulse is long, i.e. $\tau \gg \tau_0$, one can solve Eq. (4) in a quasi-static approximation. Oscillations are only weakly excited and cleaning force always balances the force from the adhesion potential:

$$\frac{1}{m}\frac{\partial U}{\partial h} \approx \ddot{l}. \tag{9}$$

Table 1
Parameters used in the calculations

Pulse duration τ[a] (ns)	11 (27 FWHM) (KrF) 2.86 (7 FWHM) (Nd–YAG) 4.2 (7 FWHM) (Nd–YAG, Gaussian)
Substrate Si	
Specific heat c (J g^{-1} K^{-1})	0.72
Volumetric thermal expansion β (K^{-1})	7.7×10^{-6}
Poisson's ratio σ	0.27
Young's modulus E (dyn cm^{-2})	1.6×10^{12}
Density ρ (g cm^{-3})	2.3
Absorption coefficient α (cm^{-1})	1.67×10^{6} (KrF); 9×10^{3} (Nd–YAG)
Absorptivity A	0.5[b], 0.39 (KrF); 0.63 (Nd–YAG)
Particle SiO_2	
Specific heat c_p (J g^{-1} K^{-1})	1
Volumetric thermal expansion β_p (K^{-1})	1.65×10^{-6}
Poisson's ratio σ_p	0.17
Young's modulus E_p (dyn cm^{-2})	0.73×10^{12}
Density ρ_p (g cm^{-3})	2.2
Work of adhesion φ (SiO_2–SiO_2) (erg cm^{-2})	68.4

[a] See Eq. (6).
[b] Value used in Figs. 3–6.

To clean, one has to overcome the biggest adhesion force during the pulse—'inertial force' cleaning regime. The force is maximal with $h = 0$ and is positive in our notations. This results in:

$$-m\ddot{l}_{\max} > F_0. \tag{10}$$

Detachment occurs in the deceleration phase [4] due to the inertia of the already accelerated particle. The same expression holds with strong damping.

Consider long ($\tau \gg \tau_0$) pulse, which ends abruptly, so that $\dot{l}$ falls from $\dot{l}_f$ to 0 within time $t_f \ll \tau_0$. During the pulse, the position h changes weakly. At the pulse end, the particle 'instantaneously' acquires 'velocity' $\dot{h} \approx -\dot{l}_f$ away from the substrate (Eq. (7)). If its kinetic energy exceeds that of adhesion, the particle will detach. This is 'kinetic energy' cleaning regime with the criterion:

$$\tfrac{1}{2}m\dot{l}_f^2 > |U_0|. \tag{11}$$

Similar considerations apply for the leading front of the pulse. In other words, to produce strong 'force', the pulse should not necessarily be short. It is enough if it has steep fronts.

We employ the potential from Eq. (1), the thermal expansion from Eq. (5), and rewrite Eqs. (8), (10), and (11) in terms of the particle radius r, pulse duration τ and fluence ϕ. This yields cleaning thresholds:

$$\phi_{cl} > 3\frac{1-\sigma}{1+\sigma}\frac{c\rho}{\beta A}\begin{cases} 0.84\left(\dfrac{2\pi\varphi}{\bar{E}}\right)^{2/3} r^{1/3}, & \tau \ll \tau_0 \\ \dfrac{3\epsilon^2}{2}\dfrac{\varphi}{\rho_p}\dfrac{\tau^2}{r^2}, & \tau \gg \tau_0 \\ \dfrac{3(2\pi)^{1/3}}{5^{1/2}}\dfrac{\varphi^{5/6}}{\rho_p^{1/2}\bar{E}^{1/3}}\dfrac{\tau}{r^{5/6}}, & \tau \gg \tau_0, \quad t_f \ll \tau_0 \end{cases} \tag{12}$$

Expansion of the particle and temporal profile of the pulse modify coefficients in Eq. (12) [8,9]. In the second expression Eq. (6) was assumed. The last expression assumes $I_f \approx \phi/\tau$.

The dependences in Eq. (12) on pulse duration τ are monotonous—shorter pulses are better. With $\tau < \tau_0$, further decrease in τ is useless. The dependence on the particle radius r is non-monotonous. There exists an optimal r for a given τ, with $\tau_0(r) \sim \tau$. With bigger r, $\tau_0(r) \gg \tau$, the cleaning force is shorter than the oscillation cycle, and cleaning proceeds in the 'elastic energy' regime. Heavy particle almost does not move during the pulse, hence the substrate surface moves faster than the center of the particle. This leads to an increase in elastic energy (compression of substrate

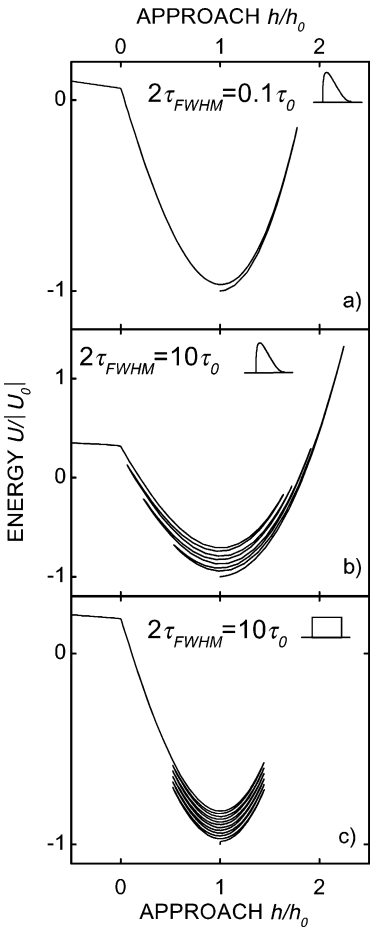

Fig. 2. Schematic movement of the particle in the adhesion potential slightly above the cleaning threshold. Laser pulse is given by Eq. (6). (a) Elastic energy cleaning regime for big particle: short pulse, $2\tau_{FWHM} = 0.1\tau_0$; (b) inertial force regime for small particle: long pulse, $2\tau_{FWHM} = 10\tau_0$; (c) kinetic energy regime for small particle: long rectangular pulse, $2\tau_{FWHM} = 10\tau_0$, and sharp fronts with $t_f \ll \tau_0$.

and particle) and detachment after the pulse. Detachment occurs in the first backward swing of oscillations (Fig. 2a). Increase in threshold is due to bigger equilibrium h_0 and adhesion energy in Eq. (2) for larger particles. With small particles $\tau_0(r) \ll \tau$, the response of the oscillator to the 'low frequency' force is inefficient. Cleaning proceeds quasi-statically, with small fast oscillations in h superimposed on the slow 'drift' in h that obeys force balance (Fig. 2b).

In the limiting case of the pulse with sharp trailing edge, the substrate stops instantaneously, while the particle continues to move—'kinetic energy' cleaning regime. It is shown in Fig. 2c for a rectangular pulse. Leading edge of the pulse gives a particle (relative) velocity towards the substrate. Resulting oscillations are unaffected by the expansion with constant velocity. Trailing edge adds velocity in the opposite direction. Kinetic energy regime is especially attractive for small particles. Its threshold has much weaker dependence on r compared to the force cleaning regime. Though our formulas refer to spherical particles, the adhesion/elasticity interplay should result in a similar behavior for arbitrary particles.

4. Influence of the pulse duration and shape, and adhesion parameters

Dependence of threshold fluence for cleaning, ϕ_{cl}, on τ and material parameters can be understood from the limiting Eq. (12). In Fig. 3, numerical results for transitional regimes are shown as well. Parameters used in the calculations are listed in Table 1. They correspond to SiO_2 particle on c-Si surface (adhesive contact is SiO_2–SiO_2). Absorptivity $A = 0.5$ is assumed. Melting thresholds estimated

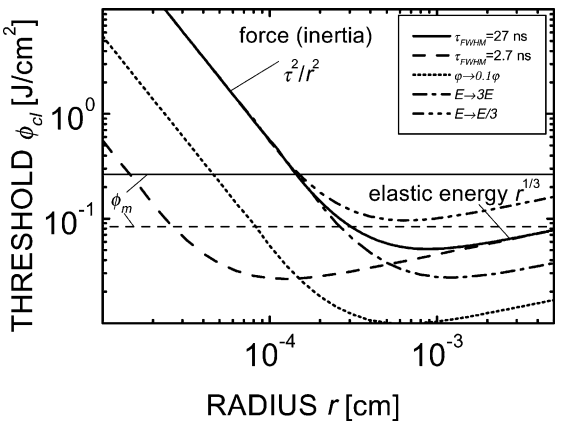

Fig. 3. Calculated influence of the pulse duration and material parameters. Laser pulse is given by Eq. (6) and parameters are listed in Table 1. Solid curve: $\tau_{FWHM} = 27$ ns; dashed curve: 10 times shorter pulse; dotted curve: 10 times weaker work of adhesion φ; dash-dotted curve: both materials are three times stiffer; dash-dot-dotted curve: both materials are three times softer. Melting thresholds for $\tau_{FWHM} = 27$ and 2.7 ns are indicated by thinner lines.

from Eq. (13) for surface absorption are shown by thinner lines:

$$\phi_{\mathrm{m}} \approx \frac{\sqrt{\pi}}{2}\frac{\Delta T_{\mathrm{m}}\, c\rho}{A}\sqrt{D\tau_{\mathrm{FWHM}}}. \qquad (13)$$

The change in τ does not influence the removal of big particles. For small particles shorter pulses are better. Damage free cleaning window shrinks with decreasing τ. Change in work of adhesion φ is more critical for smaller particles, as expected from Eq. (12). If both materials are taken stiffer/softer by changing their Young's modules, this does not affect (inertial) removal of small particles, but makes elastic removal better/worse.

Fig. 4 shows how kinetic energy cleaning regime arises. The pulse given by Eq. (6) is cut at the point of maximum intensity $t = \tau$ with a 100 ps shutter. The results for the first and second part of such a pulse demonstrate slope corresponding to a kinetic regime for small particles. The difference is due to different FWHM. Kinetic regime allows one to increase damage free cleaning window.

Thin curves refer to a rectangular pulse with the same FWHM. Two curves differ in rise/fall time t_{f}. With $t_{\mathrm{f}} = 1$ ns, small particles again follow force cleaning regime—such t_{f} is too large for them. The origin of oscillations in $\phi_{\mathrm{cl}}(r)$ dependence is clarified by Fig. 2c. If the trailing edge of the pulse arrives at the right time, detachment is facilitated. Similar, but less pronounced effect can be seen for the first part of the pulse given by Eq. (6). It is absent for the second part, as here the steep leading edge alone determines detachment condition.

5. Resonance effects

Existence of internal frequency for the adhering particle suggests that resonant effects can be employed to improve cleaning. Resonance does not allow one to decrease cleaning threshold below that of a very short pulse with the same fluence. But it permits one to use modulated pulses that are longer, and therefore, have higher damage threshold, without significant loss of efficiency. This should increase damage free cleaning window. Consider sinusoidally modulated intensity:

$$I = I_0(1-\cos(2\pi\nu_l t)), \quad I \equiv 0, \quad \text{for } \nu_l t > N_l. \qquad (14)$$

Calculated threshold for $N_l = 10$ such pulses is shown in Fig. 5. Here, ϕ is the overall fluence in the pulse train, as it determines the damage threshold estimated from the Eq. (13) using total duration of the pulse train $\tau_{\mathrm{FWHM}} \to \tau_{\mathrm{total}} = N_l/\nu_l$. Melting fluences are shown

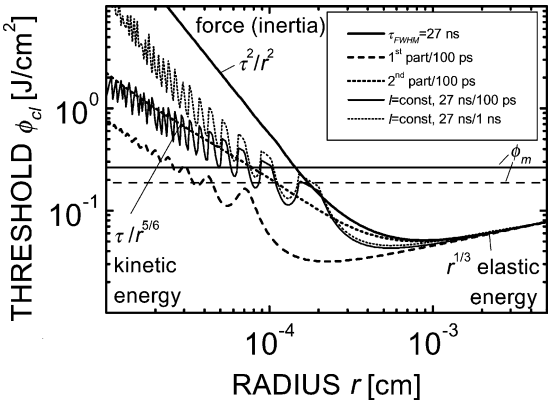

Fig. 4. Influence of the pulse shape. Laser pulse with $\tau_{\mathrm{FWHM}} = 27$ ns is given by Eq. (6). Solid curve: full pulse; dashed curve: first part of the pulse cut with $t_{\mathrm{f}} = 100$ ps; dotted curve: second part of the pulse; thinner curves: rectangular pulse, $\tau_{\mathrm{FWHM}} = 27$ ns; thin solid curve: $t_{\mathrm{f}} = 100$ ps; thin dotted curve: $t_{\mathrm{f}} = 1$ ns. Melting thresholds for $\tau_{\mathrm{FWHM}} = 27$ and 13.5 ns are indicated by thinner straight lines.

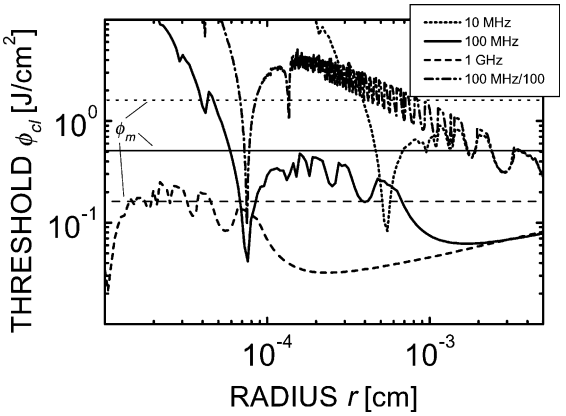

Fig. 5. Resonance effects for 10 sinusoidal pulses (Eq. (14)). Parameters are listed in Table 1. Circular frequency of oscillations ν_l for each curve is given in the legend. Melting thresholds are indicated by thinner lines. Dash-dotted line refers to a train of 100 pulses.

by straight lines for each repetition frequency (i.e. overall pulse duration). Large-scale behavior of $\phi_{cl}(r)$ resembles that of a single pulse. But if the frequency of modulation is in resonance with adhesion frequency, ϕ_{cl} drops sharply.

The number of oscillations N_l should not be large. Due to non-linearity of potential in Eq. (1), resonant minimum corresponds to $\tau_0(r) \approx 1.1/\nu_l$, not to linear $\tau_0(r) = 1/\nu_l$ expression, and resonance saturates even without damping. Dash-dotted curve shows the threshold for 100 oscillations with 100 MHz. Resonance is much narrower and will be smeared out by the dispersion in parameters. Damage threshold in this case coincides with dotted damage threshold line, i.e. damage free cleaning window is smaller for 10 oscillations. This window narrows also for higher frequencies, but as dashed curve (1 GHz) illustrates, resonance may allow one to clean particles, which otherwise would have been impossible to remove.

The situation is even more promising for rectangular modulation (with 50% duty ratio). In the same notations as in Eq. (14) with I_0 being the average intensity

$$I = \begin{cases} 2I_0, & n < \nu_l t < n + \frac{1}{2} \\ 0, & n + \frac{1}{2} < \nu_l t < n + 1 \end{cases} \qquad (15)$$

where $n = 0, \ldots, N_l - 1$. Train of rectangular pulses combines resonant influence with the advantage of kinetic energy cleaning regime due to the presence of steep fronts (Fig. 6). Their rise/fall time t_f (time constant of a shutter) is indicated in the legend after a slash. Calculations are presented mainly for $t_f = 100$ ps, which is short enough to ensure kinetic energy cleaning regime. For small particles, $\phi_{cl}(r)$ dependence is weaker than in Fig. 5 due to the difference between force and kinetic energy cleaning regimes in Eq. (12). Dash-dotted curve for 100 MHz illustrates that as in Fig. 4, shutter time of 1 ns is not short enough to ensure kinetic energy regime for small particles. Dash-dot-dotted curve corresponds to $t_f = 10$ ps and almost coincides with 100 ps curve. Comparing Figs. 5 and 6, we see that for particles bigger than resonant ones, there is little difference between sinusoidal and rectangular modulation. For smaller particles, steep fronts of rectangular modulation make secondary resonances more pronounced and decrease thresholds. Thus, rectangular modulation should be preferred, unless this complicates technical realization.

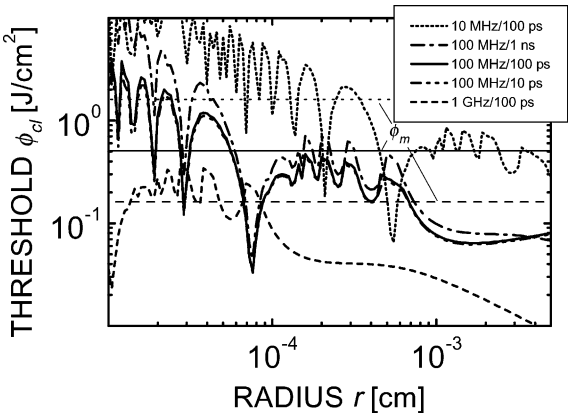

Fig. 6. Calculated resonance effects for 10 rectangular pulses (Eq. (15)). Frequency of oscillations and t_f are given in the legend. Melting thresholds are indicated by thinner lines.

For the practical implementation, it is important that fluences considered in Figs. 5 and 6 imply high intensities. Thus, with CW lasers with power $P \sim 1$ W, tight focusing (several μm) is required. CW lasers with $P \sim 100$ W are less restrictive. Other possibilities include: fast modulation of pulsed (e.g. excimer) lasers, splitting of the pulse and usage of optical delay lines to produce pulse train, usage of mode locking with moderate (5–10) number of locked modes. Comparison of experimental results for cleaning of SiO_2 particles from Si will be presented elsewhere.

6. Conclusions

We considered the DLC problem with nanosecond pulses as an escape from the adhesion potential under the action of a cleaning force related to thermal expansion. Besides pull-out force F_0, the parameters of the adhesion potential most important for DLC are the period of oscillations τ_0 and equilibrium deformation h_0. The laser pulse duration τ should be compared with τ_0, and the overall thermal expansion l with h_0. Expressions for the cleaning threshold ϕ_{cl} are derived. With $\tau < \tau_0$ (big particles) cleaning takes place in the 'elastic energy' regime, which requires $l > h_0$ resulting in $\phi_{cl} \propto r^{1/3}$. With $\tau > \tau_0$ (small particles), cleaning occurs in the 'inertial

force' regime, which requires decelerations $-m\ddot{l}_{\max} > F_0$, leading to $\phi_{\mathrm{cl}} \propto \tau^2/r^2$. With $\tau > \tau_0$, but steep edges of the pulse $t_{\mathrm{f}} \ll \tau_0$, cleaning requires that particle kinetic energy exceeds that of adhesion $m\dot{l}_{\mathrm{f}}^2/2 > |U_0|$. This leads to $\phi_{\mathrm{cl}} \propto \tau/r^{5/6}$ for the 'kinetic energy' regime. This increases damage free cleaning window for small particles. Utilization of resonance effects by modulation of laser pulses is suggested. The results are easily generalized to the case of absorbing particle or when both materials absorb [8,9].

Acknowledgements

We thank Prof. D. Bäuerle, Dr. M. Mosbacher, and Prof. B. Luk'yanchuk for useful discussions. Financial support by the EU TMR project Laser Cleaning no. ERBFMRXCT98 0188, and the Fonds zur Förderung der wissenschaftlichen Forschung in Österreich project P14700-TPH is gratefully acknowledged.

References

[1] W. Zapka, W. Ziemlich, A.C. Tam, Appl. Phys. Lett. 58 (1991) 2217.
[2] The National Technology Roadmap for Semiconductors, Semiconductors Industry Association, San Jose, CA, 1994.
[3] D. Bäuerle, Laser Processing and Chemistry, 3rd Edition, Springer, Berlin, 2000.
[4] V. Dobler, R. Oltra, J.P. Boquillon, M. Mosbacher, J. Boneberg, P. Leiderer, Appl. Phys. A 69 (1999) 335.
[5] Y.F. Lu, W.D. Song, B.W. Ang, M.H. Hong, D.S.H. Chan, T.S. Low, Appl. Phys. A 65 (1997) 9.
[6] V.P. Veiko, E.A. Shakhno, S.V. Nikolaev, Proc. SPIE 4088 (2000) 179.
[7] Y.F. Lu, Y.W. Zheng, W.D. Song, Appl. Phys. A 68 (1999) 569.
[8] N. Arnold, G. Schrems, T. Mühlberger, M. Bertsch, M. Mosbacher, P. Leiderer, D. Bäuerle, Proc. SPIE 4426 (2002) 340.
[9] N. Arnold, in: B. Luk'yanchuk (Ed.), Laser Cleaning, World Scientific, Singapore, 2001, Chapter 2.
[10] B. Luk'yanchuk, Y.W. Zheng, Y.F. Lu, Proc. SPIE 4423 (2001) 115.
[11] G. Vereecke, E. Röhr, M.M. Heyns, J. Appl. Phys. 85 (1999) 3837.
[12] L.D. Landau, E.M. Lifshitz, Theory of Elasticity, Pergamon Press, New York, 1986, pp. 6–7.